Structural and Vibrational Properties of Three Species of Anti-Histaminic Diphenhydramine by Using DFT Calculations and the SQM Approach

Silvia Antonia Brandán*, Maximiliano A. Iramain

[1]Cátedra de Química General, Instituto de Química Inorgánica, Facultad de Bioquímica. Química y Farmacia, [2]Universidad Nacional de Tucumán, Ayacucho 471, (4000) San Miguel de Tucumán, Tucumán, Argentina.

sbrandan@fbqf.unt.edu., miramain9@gmail.com

Abstract

In the present work, the free base, cationic and hydrochloride species of the anti-histaminic diphenhydramine drug were theoretically studied by using the hybrid B3LYP/6-311++G** calculations in the gas phase and the experimental available infrared and Raman spectra for the hydrochloride form in the solid phase. Here, the 114, 117 and 120 vibration normal modes expected for the free base, cationic and hydrochloride species of DPH, respectively were reported together with their corresponding force fields at the same level of theory. The atomic NPA and Mulliken charges, molecular electrostatic potentials, bond orders, main delocalization energies and topological properties were studied for those three species of DPH. The results show that the cationic species presents the higher dipole moment value, as expected because this species is charged while the presence of Cl atom justifies the higher volume observed for the hydrochloride species. Very good correlations were found between the theoretical and experimental available geometrical parameters for the hydrochloride species of DPH. The NBO and AIM analyses show the high stability of the hydrochloride species due to the presence of one H bond and two halogen bonds different from only one H bond observed in other two species of DPH. The evaluations of the frontier orbitals show that the hydrochloride form is the most reactive due to its low gap value while the cationic form is the less reactive. The comparisons of the gap values for the three species of DPH with other similar species containing the N-CH_3 groups, such as the tropane, cocaine and morphine alkaloids, have showed that the three species of DPH have practically the same reactivities while in the three forms of those alkaloids the values are very different among them, presenting the three forms of tropane the lowest reactivities. Hence, the three species of DPH, with two N-CH_3 groups, have apparently the same reactivities than the cationic form of cocaine. Finally, the vibrational analyses for the three species of DPH evidence that the presence of two halogen bonds and one H bond in the hydrochloride species of DPH, due to the Cl atom, produce a shifting of deformation βR_1(A1) ring mode of a ring with respect to the other βR_1(A2) while in the free base and cationic the deformation rings modes of both rings are predicted at the same wavenumbers.

Keywords: Diphenhydramine, Vibrational Spectra, Molecular Structure, Descriptor Properties, DFT Calculations.

Diphenhydramine is an anti-histaminic drug used from long time in the treatment of multiple diseases [1-21] and when it is used in combination with others species in formulated preparations their properties and uses notably increase [4,8,10,11,14-16]. Three different structures are expected for diphenhydramine due to the presence of a tertiary amine, these are, their free base, cationic and hydrochloride forms, being the IUPAC name of the commercial species 2-benzhydryloxy-N, N-dimethylethanamine hydrochloride. The structure of the hydrochloride form was already determined by using X-ray crystallography studies and CP-MAS ^{13}C-NMR spectroscopy by Glaser and Maartmann-Moe [1]. The study of their structures and properties are very important to know the most stable conformers, reactivities in the different media and also, to identify diphenhydramine alone or combined in a mixture. Usually, the dosage of the pharmaceutical mixtures and their qualitative and quantitative determinations are normally carried out by using different techniques, being the most used the spectroscopic ones [1,2,4,8-11,16,17]. Due to the cardio-respiratory side effects that present diphenhydramine the knowledge of new products is very important for the design of species with low effects and better pharmacological properties [6,7,12,13,18-21]. On the other hand, the presence of two N-CH_3 groups in the three

* Corresponding author. Tel.: +54-381-4247752; fax: +54-381-4248169;
E- mail: sbrandan@fbqf.unt.edu.ar (S.A. Brandán).

different forms of diphenhydramine, similar to the tropane derivatives where are observed only a group, are of structural interest taking into account that in different media and temperature the N-CH_3 group can undergo fast N-methyl inversion [22]. In this context, here we have presented a structural and vibrational study of the three species of diphenhydramine in gas phase by using calculations based on the density functional theory (DFT) and their experimental available infrared spectrum. Here, the properties of those three species were predicted and the complete assignments of their vibrational spectra were reported. All calculations were performed with the hybrid B3LYP/6-311++G** method [23,24] while the scaled quantum mechanical force field (SQMFF) approach [25] and the Molvib program [26] were used to calculate the harmonic force fields and to perform the complete vibrational assignments of those three species of diphenhydramine. The structural properties, such as the atomic charges, bond orders, molecular electrostatic potentials, donor-acceptor interactions energies and the topological properties were predicted for those three species by using the natural bond orbital (NBO) and atoms in molecules (AIM) calculations at the same level of theory [27,28]. In addition, the reactivities of those three species and their behaviors in gas phase were predicted at the same level of theory by using the frontier orbitals and different descriptors, as suggested by Parr and Pearson [29-36]. Finally, these parameters obtained here for the free base, cationic and hydrochloride forms of diphenhydramine were compared with those obtained for tropane, cocaine and morphine alkaloids taking into account the presence of a similar N-CH_3 group in the structures of those alkaloids [37-39].

Computational details

The structures of free base, cationic and hydrochloride forms of diphenhydramine (DPH) were built with the *GaussView* program [40]. First, the free base was modelled and later to this structure was added an H atom forming the cationic species and, later to the cationic species was added the Cl atom forming, this way, the hydrochloride species. Then, the three species were optimized by using the hybrid B3LYP/6-311++G** level of theory with the Gaussian 09 program [41]. Here, the potential energy surfaces (PES) were studied performing only variations on the dihedral N2-C7-C6-O1 and C7-C6-O1-C3 angles by using the same level of theory. Here, the curve for the dihedral N2-C7-C6-O1 angle clearly shows two structures with local minima and only one with a global minimum, as expected. Therefore, these most stable structures were considered for those three species where the dihedral N2-C7-C6-O1 angles have a value of -66°.

Figure 1 shows the most stable theoretical structures for those three species of DPH.

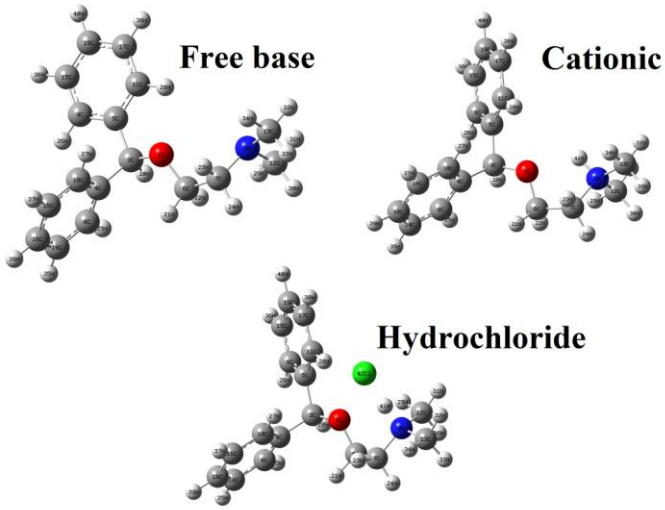

Figure 1. Molecular structures of the most stable conformers of free base, cationic and hydrochloride forms of diphenhydramine and atoms numbering.

Here, the structural properties computed for the three species in gas phase were the charges, atomic natural populations (NPA) and MK (Merz-Kollman) charges, the molecular electrostatic potentials (MEP), the bond

orders, the acceptor-donor interactions energies and the topological properties [27,28,42]. On the other side, the harmonic force fields for those three species were also calculated taking into account their normal internal coordinates by using the SQMFF approach [25] and the Molvib program [26]. The vibrational assignments were performed considering for those species Potential Energy Distribution (PED) contributions $\geq$10% and comparing their predicted vibrational spectra with that experimental available for the hydrochloride form of DPH in the solid phase. Here, a better approximation between theoretical and experimental spectra can be seen when the predicted the Raman spectrum expressed in activities were converted to intensities by using known equations [43,44]. The predictions of reactivities and behaviours for the free base, cationic and hydrochloride forms of DPH in the gas phase were carried out by using the gap values calculated from the frontier orbitals. After that, using the corresponding gap values for each species the chemical potential (μ), electronegativity (χ), global hardness (η), global softness (S), global electrophilicity index (ω) and global nucleophilicity index (E) descriptors were computed by using the equations reported in the literature [29-36]. In particular, these results were compared with those obtained for known alkaloids which contain the same N-CH_3 group and, for these reasons, the same free base, cationic and hydrochloride structures [37-39].

Results and discussion

Structural studies in gas phase

Table 1 shows the calculated total energies, dipole moments, volume values free Base, cationic and hydrochloride in gas phase by using the B3LYP/6-311++G** method. Clearly, it is observed that the cationic form presents the higher dipole moment value, as expected, because this species is charged, in relation to the other two neutral species. Besides, we observed that the hydrochloride species has the higher volume; the witch is obviously, due to the presence of the Cl atom.

Table 1. Calculated total energy (E), dipolar moment (μ) and volume for the Free Base, Cationic and Diphenhydramine Hydrochloride in gas phase.

B3LYP/6-311++G**method			
Gas Phase			
Conformers	E	μ	V
Free base	-790.6156	1.58	297.6
Cationic	-791.0085	12.54	304.4
Hydrochloride	-1251.4728	8.92	328.6

Comparisons of calculated geometrical parameters for the free base, cationic and hydrochloride species of DPH in gas phase by using the B3LYP/6-311++G** method with those experimental ones available for hydrochloride by X-ray diffraction [1] are presented in **Table 2**. These comparisons are expressed as the differences between calculated and experimental values by means of the root-mean-square deviation (RMSD) values. Hence, we observed very good agreements for bond lengths and angles when these theoretical parameters are compared with those experimental available for the hydrochloride species [1] while the higher deviations are observed in the dihedral angles. Thus, RMSD values between 0.055 and 0.049 Å are observed for bond lengths while for bond angles are observed values between 4.2 and 2.9 °. Then, the higher differences in the RMSD values are observed for dihedral angles (114.4-64.5 °) where clearly the hydrochloride species present the better correlation, as expected because both species compared are the same, as observed in **Figure 2**. The identifications of their rings can be seen in the same figure.

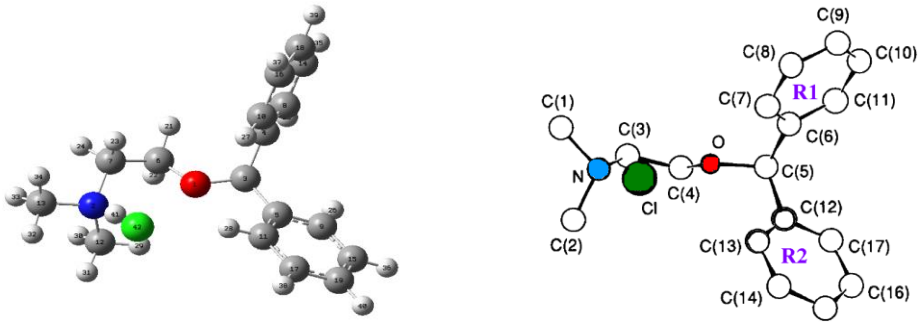

Figure 2. Comparison between the theoretical structure for the hydrochloride DPH with the corresponding experimental one from Ref [1].

On the other hand, for all species, the calculated values are underestimated in relation to the experimental ones and, in particular, for the three species of DPH the predicted N2-C12 and N2-C13 distances are lower than the other N2-C7 one, a result different from that experimental value obtained for the hydrochloride species because the bond N2-C7 length (1.431 Å) in this species present a low value than the other two N2-C12 and N2-C13 distances of 1.449 and 1.452 Å, respectively. Another very important result we observed in the C6-O1 and C3-O1 distances because the bond C6-O1 length experimentally observed is of 1.279 Å for the hydrochloride species, a value slightly low than those predicted for the three species (1.419-1.408 Å) by using B3LYP/6-311++G** calculations. In reference to the bond angles there are very good correlations in the C4-C8-C14 and C5-C9-C15 angles for the three species with that experimentally observed for the hydrochloride species while for the C4-C3-C5 angle between both rings the (113.4-112.7 °) values in the three species are underestimated, in relation to that experimental one (110.4 °). When the dihedral angles are analyzed exhaustively we observed that the calculations predicted in the three species the dihedral C13-N2-C7-C6 angles underestimated in reference to that experimental (143.3 °) while on the contrary are observed for the other dihedral C12-N2-C7-C6 angles.

Table 2. Comparison of calculated geometrical parameters for the Free Base, Cationc and Diphenhydramine Hydrochloride in gas phase compared with the experimental available by X-ray for hydrochloride DPH.

B3LYP method 6-311++G**				Experimental
Parameters	Gas phase			
	Free base	Cationic	HCl	Exp[b]
Bond lengths (Å)				
C5-C11	1.397	1.398	1.397	1.391
C11-C17	1.394	1.394	1.395	1.374
C17-C19	1.393	1.393	1.393	1.372
C19-C15	1.394	1.393	1.394	1.372
C15-C9	1.392	1.392	1.392	1.408
C9-C5	1.399	1.397	1.398	1.368
C5-C3	1.527	1.515	1.520	1.465
C3-C4	1.524	1.519	1.525	1.512
C4-C10	1.399	1.400	1.400	1.384
C10-C16	1.391	1.391	1.391	1.395
C16-C18	1.396	1.396	1.396	1.353
C18-C14	1.391	1.391	1.392	1.378
C14-C8	1.396	1.395	1.396	1.409
C8-C4	1.395	1.397	1.395	1.369
C3-O1	1.423	1.461	1.434	1.418
O1-C6	1.419	1.41	1.408	1.279

C6-C7	1.521	1.525	1.521	1.389
C7-N2	1.460	1.517	1.497	1.431
N2-C12	1.455	1.499	1.483	1.449
N2-C13	1.456	1.497	1.486	1.452
Cl42---N2			2.877	2.990
RMSD[a]	**0.049**	**0.054**	**0.055**	
Bond Angles (°)				
C3-O1-C6	114.6	115.8	115.0	122.9
C7-N2-C12	112.9	112.8	115.3	113.0
C7-N2-C13	111.4	112.5	110.2	106.6
C12-N2-C13	111.1	111.6	111.5	111.3
O1-C3-C4	111.6	111.1	110.8	110.4
O1-C3-C5	107.9	107.1	107.9	110.0
C4-C3-C5	113.4	114.9	112.7	110.4
C3-C4-C8	120.9	119.5	120.7	120.9
C3-C4-C10	120.0	121.4	120.1	120.3
C8-C4-C10	118.9	118.9	119.0	118.3
C3-C5-C9	120.3	118.8	118.9	120.9
C3-C5-C11	120.6	122.1	121.5	120.1
C9-C5-C11	118.9	119.0	119.4	118.9
O1-C6-C7	109.1	104.9	109.1	118.7
N2-C7-C6	114.9	109.1	115.4	119.8
C4-C8-C14	120.7	120.6	120.6	120.2
C5-C9-C15	120.6	120.6	120.5	120.2
C4-C10-C16	120.4	120.3	120.3	122.1
C5-C11-C17	120.3	120.3	119.8	121.0
C8-C14-C18	119.9	119.9	119.9	121.4
C9-C15-C19	120.1	120.0	119.9	119.6
C10-16-C18	120.2	120.2	120.3	119.7
C11-C17-	120.4	120.2	120.6	119.9
C14-C18-	119.6	119.8	119.7	119.2
C15-19-C17	119.4	119.6	119.6	120.4
RMSD[a]	**3.0**	**4.2**	**2.9**	
Diedral Angles (°)				
C13-N2-C7-	162.2	155.1	167.6	143.3
C12-N2-C7-	-71.7	-77.3	-40.1	-93.1
N2-C7-C6-	-67.1	-44.3	-50.6	-38.1
C7-C6-O1-	-177.7	-177.4	-	-170.2
C6-O1-C3-	-162.3	-170.5	-	-106.2
C6-O1-C3-	72.3	63.0	71.4	131.7
O1-C3-C5-	166.3	145.0	157.8	38.5
O1-C3-C5-	-16.3	-36.4	-23.2	-142.9
O1-C3-C4-	-124.8	-116.4	-	-33.4
O1-C3-C4-	54.7	63.5	52.3	152.4
C3-C5-C11-	-177.1	-178.4	-	-177.0
C3-C5-C9-	177.5	178.1	178.6	177.4
C3-C4-C8-	-179.9	-179.5	-	-173.3
C3-C4-C10-C16	-179.7	-179.9	179.6	173.5
RMSD[a]	**114.4**	**110.8**	**64.5**	

[a]This work; [b]From Ref. [1]; RMSD, in letter bold.

Hence, the values predicted in the three species are between -40.1 and -77.3 ° while the experimental one is -93.1 °. In general, the geometrical parameters calculated for the free base, cationic and hydrochloride species

by using the B3LYP/6-311++G** method show reasonable correlations when are compared with those experimental determined to the hydrochloride species. Therefore, the vibrational studies for those three species can easily be performed with those theoretical structures predicted by using that basis set.

NPA and Mulliken Charges, molecular electrostatic potentials and bond orders studies

For the three species of DPH, the atomic natural population (NPA) and Mulliken charges were studied by using the B3LYP/6-311++G** method in the gas phase. These results are summarized in **Table 3**. Firstly, we observed that the NPA charges present higher values than the Mulliken ones and, in general, the higher values are observed on all atoms of the cationic species. For all species it is interesting to compare both charges on the O1, N2 and C3, C6, C7, C12 and C13 atoms because these atoms are related to the C3-O1 and C6-O1 bond lengths and to the two N2-CH_3 groups whose predicted distances, as was above analyzed, are slightly different among them. Thus, when the values of Mulliken and NPA charges on those mentioned atoms are graphed in function of the atoms belonging to the three species very important differences are observed only in the Mulliken charges, as can be seen in **Figure 3**. Evidently the higher differences are observed in the Mulliken's charges on the N2 atom of the free base because presents a negative value while in the other two species that atom present positive values, showing the higher value the hydrochloride species. Other important differences are observed on the C3 atoms because in the free base that atom has positive sign while in the other two species these atoms have negative values. Note that the NPA charges on the C3 atoms in the three species present positive signs while the O1 atoms have the most negative values in the three species. From this study and evaluating only the charges on the O1, N2 and C3, C6, C7, C12 and C13 atoms, it is clearly observed that the effect of to add an H atom to the free base is to change the sign and increase the value of the Mulliken charge on the N2 atom and, simultaneously, to increase the negative charges on the O1, C12 and C13 atoms. On the contrary, the effect of to add a Cl atom to the cationic species is to increase the charges on the N2 (positive) and C13 (negative) atoms and, to decrease the negative charges on the O1 and C12 atoms.

Other interesting properties studied in the three species of DPH are the molecular electrostatic potential, calculated (MEP) from the Merz-Kollman charges [45], and the bond orders, expressed as Wiberg indexes. These results for the free base, cationic and hydrochloride species of diphenhydramine in gas phase by using the B3LYP/6-311++G** method can be observed in **Table 4**. Analyzing carefully the MEP values for the three species we observed that on all atoms corresponding to the free base are predicted the higher values, having the O atoms, in the free base and in the cationic species, the highest values because these atoms are the most electronegative while in the hydrochloride species the Cl atom has the highest value, as expected. The MEP values on all atoms present practically the same behaviours than the studied charges, thus, its values decrease from the free base to the cationic species while increase in the hydrochloride one.

Table 3. Mulliken and NPA charges observed on all atoms for the Free Base, Cation and Hydrochloride species of Diphenhydramine in gas phase by using B3LYP/6-311++G** level of theory.

Atoms	B3LYP/6-311++G**[a]			Atoms			
	Mulliken´s charges				NPA charges		
	Free	Cation	HCl		Free	Cation	HCl
O1	-0.336	-0.391	-0.166	O1	-0.601	-0.640	-0.606
N2	-0.113	0.164	0.461	N2	-0.553	-0.450	-0.544
C3	0.051	-0.172	-0.495	C3	0.119	0.127	0.124
C4	0.188	0.324	0.323	C4	-0.056	-0.087	-0.062
C5	0.109	0.249	0.413	C5	-0.042	-0.062	-0.053
C6	0.086	0.180	0.176	C6	-0.023	-0.045	-0.036
C7	-0.015	-0.188	-0.168	C7	-0.180	-0.172	-0.174
C8	-0.204	-0.281	-0.188	C8	-0.204	-0.196	-0.205
C9	-0.253	-0.291	-0.354	C9	-0.203	-0.190	-0.202
C10	-0.073	-0.190	-0.130	C10	-0.187	-0.192	-0.189
C11	-0.040	-0.226	-0.294	C11	-0.197	-0.212	-0.202

C12	-0.301	-0.477	-0.431	C12	-0.356	-0.354	-0.360
C13	-0.397	-0.413	-0.472	C13	-0.350	-0.350	-0.350
C14	-0.119	-0.084	-0.155	C14	-0.200	-0.189	-0.199
C15	-0.098	-0.038	-0.020	C15	-0.198	-0.182	-0.201
C16	-0.178	-0.116	-0.151	C16	-0.196	-0.186	-0.192
C17	-0.158	-0.090	-0.061	C17	-0.196	-0.189	-0.187
C18	-0.142	-0.138	-0.144	C18	-0.203	-0.182	-0.201
C19	-0.155	-0.168	-0.224	C19	-0.208	-0.189	-0.206
H20	0.073	0.137	0.182	H20	0.178	0.184	0.176
H21	0.014	0.057	0.014	H21	0.172	0.218	0.196
H22	0.053	0.030	0.013	H22	0.158	0.174	0.163
H23	0.088	0.141	0.123	H23	0.203	0.224	0.227
H24	0.036	0.142	0.073	H24	0.165	0.226	0.198
H25	0.103	0.136	0.110	H25	0.202	0.204	0.199
H26	0.136	0.151	0.151	H26	0.209	0.208	0.198
H27	0.096	0.132	0.127	H27	0.216	0.210	0.226
H28	0.050	0.131	0.216	H28	0.229	0.203	0.254
H29	0.117	0.218	0.183	H29	0.189	0.226	0.230
H30	0.088	0.207	0.129	H30	0.158	0.220	0.191
H31	0.127	0.201	0.171	H31	0.194	0.227	0.220
H32	0.155	0.194	0.200	H32	0.191	0.226	0.226
H33	0.109	0.190	0.138	H33	0.158	0.221	0.190
H34	0.138	0.185	0.178	H34	0.193	0.226	0.222
H35	0.126	0.141	0.136	H35	0.204	0.216	0.205
H36	0.121	0.132	0.103	H36	0.202	0.216	0.202
H37	0.134	0.139	0.136	H37	0.205	0.215	0.208
H38	0.131	0.134	0.129	H38	0.202	0.211	0.210
H39	0.129	0.145	0.132	H39	0.205	0.217	0.205
H40	0.126	0.148	0.136	H40	0.202	0.216	0.202
H41		0.254	-0.086			0.452	0.424
Cl42			-0.617				-0.726

[a]This work

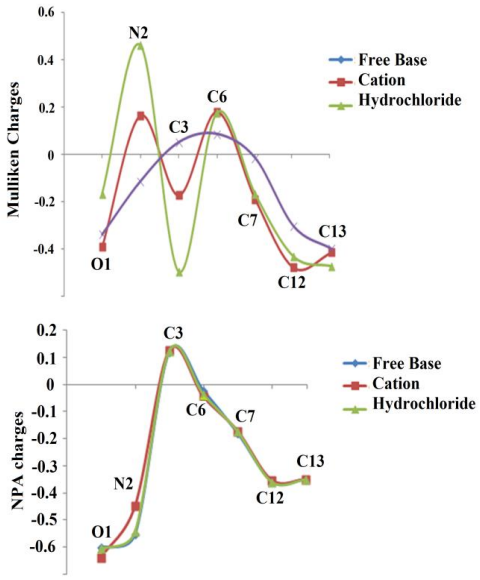

Figure 3. Calculated Mulliken (upper) and NPA (bottom) charges on the atoms corresponding to the free base, cationic and hydrochloride species of diphenhydramine in gas phase by using the B3LYP/6-311++G** Method.

The bond order (BO), expressed by the Wiberg index is other interesting property studied for the three species of DPH. These results for the free base, cationic and hydrochloride species in gas phase by using the B3LYP/6-311++G** method are given in Table 4. The values show a higher double bond characters in the O atoms belonging to the free base and hydrochloride species while the character slightly decrease in the cationic species. When the results of BO are analyzed for the N2 atoms in the three species the cationic species present the higher value, then the hydrochloride species and, finally the free base, as can be easily seen in **Figure 4**. Later, evaluating the BO values only for the C7, C12 and C13 atoms linked to the N2 atoms we observed practically similar behaviors, as shown in Figure 4.

Table 4. Molecular Electrostatic Potential and Wiber indexes for the free Base, cationic and hydrochloride of diphenhydramine in gas phase by using B3LYP/6-311++G** level of theory.

Atoms	Molecular Electrostatic Potential			Wiberg Index		
	Free base	Cationic	HCl	Free base	Cationic	HCl
O1	-22.368	-22.219	-22.348	O1	2.014	1.975
N2	-18.404	-18.117	-18.296	N2	3.119	3.474
C3	-14.708	-14.590	-14.699	C3	3.895	3.866
C4	-14.766	-14.666	-14.761	C4	4.013	4.012
C5	-14.770	-14.664	-14.771	C5	4.011	4.010
C6	-14.726	-14.570	-14.693	C6	3.836	3.821
C7	-14.749	-14.561	-14.700	C7	3.908	3.827
C8	-14.770	-14.676	-14.767	C8	3.965	3.964
C9	-14.781	-14.680	-14.780	C9	3.959	3.962
C10	-14.774	-14.678	-14.773	C10	3.959	3.961
C11	-14.786	-14.677	-14.792	C11	3.952	3.962
C12	-14.758	-14.565	-14.713	C12	3.857	3.768
C13	-14.759	-14.565	-14.713	C13	3.853	3.764
C14	-14.770	-14.682	-14.768	C14	3.967	3.962
C15	-14.780	-14.684	-14.782	C15	3.967	3.962
C16	-14.772	-14.682	-14.770	C16	3.966	3.963
C17	-14.782	-14.682	-14.788	C17	3.967	3.964
C18	-14.771	-14.683	-14.769	C18	3.967	3.961
C19	-14.781	-14.686	-14.785	C19	3.967	3.962
H20	-1.113	-0.997	-1.103	H20	0.973	0.970
H21	-1.121	-0.968	-1.087	H21	0.975	0.955
H22	-1.118	-0.967	-1.091	H22	0.978	0.973
H23	-1.120	-0.936	-1.078	H23	0.962	0.952
H24	-1.122	-0.928	-1.068	H24	0.976	0.951
H25	-1.103	-1.009	-1.098	H25	0.962	0.961
H26	-1.114	-1.013	-1.111	H26	0.960	0.959
H27	-1.111	-1.013	-1.111	H27	0.957	0.959
H28	-1.125	-1.010	-1.134	H28	0.954	0.962
H29	-1.121	-0.929	-1.079	H29	0.967	0.951
H30	-1.126	-0.929	-1.072	H30	0.979	0.953
H31	-1.121	-0.930	-1.075	H31	0.965	0.950
H32	-1.122	-0.930	-1.078	H32	0.966	0.950
H33	-1.128	-0.929	-1.073	H33	0.979	0.953
H34	-1.122	-0.930	-1.077	H34	0.965	0.950
H35	-1.105	-1.020	-1.102	H35	0.961	0.955
H36	-1.114	-1.022	-1.115	H36	0.961	0.955

H37	-1.107	-1.020	-1.107	H37	0.960	0.956
H38	-1.117	-1.019	-1.125	H38	0.962	0.958
H39	-1.106	-1.022	-1.104	H39	0.960	0.955
H40	-1.115	-1.023	-1.118	H40	0.961	0.955
H41		-0.824	-0.997	H41		0.799
Cl42			-64.526	Cl42		

Values in a.u.

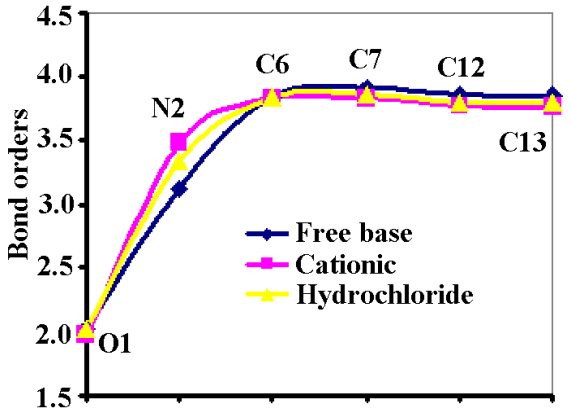

Figure 4. Calculated Bond orders for the atoms corresponding to the free base, cationic and hydrochloride species of diphenhydramine in gas phase by using the B3LYP/6-311++G** Method.

NBO and AIM studies

For the three-different species of DPH were performed NBO and AIM calculations [27,28] because the study of their stabilities are of great interest to know which of those species is the most stable present in the gas phase. Hence, the main delocalization energies calculated by using the B3LYP/6-311++G** level of theory from the NBO program [27] are summarized for each species in **Table 5**.

Table 5. Main delocalization energies (in kJ/mol) for the Free Base. Cationic and Diphenhydramine Hydrochloride in gas phase by using B3LYP/6-311++G** level of theory.

Delocalization	B3LYP/6-311++G**		
	Free base	Cationic	HCl
*πC4-C8→ π*C10-*	80.46	79.96	79.21
*πC4-C8→ π*C14-*	84.69	77.25	83.98
*πC5-C9→ π*C11-*		83.18	
*πC5-C9→ π*C15-*		81.38	
*πC5-C11→ π*C9-*	86.11		88.45
*πC5-C11→ π*C17-*	89.86		84.18
*πC9-C15→ π*C5-*	85.10		83.60
*πC9-C15→ π*C17-*	83.64		80.92
*πC10-C16→ π*C4-*	88.16	88.57	88.99
πC10-C16→	86.02	82.10	86.48
*πC11-C17→ π*C5-*		89.37	
πC11-C17→		79.75	
*πC14-C18→ π*C4-*	81.55	90.12	82.47
πC14-C18→	80.88	83.14	80.26
*πC15-C19→ π*C5-*		89.54	

$\pi C15\text{-}C19 \rightarrow$		89.45	
$\pi C17\text{-}C19 \rightarrow \pi^*C5\text{-}$	83.01		83.81
$\pi C17\text{-}C19 \rightarrow \pi^*C9\text{-}$	85.73		88.36
$\pi^*C9\text{-}C15 \rightarrow \pi^*C5\text{-}C11$			1068.78
$\Delta E_{\pi \rightarrow \pi^*}$	**1015.21**	**1013.81**	**2079.49**

That table shows interesting results for the three species, as a consequence of the di-phenyl rings. In fact, all contributions are transitions from bonding to antibonding orbitals and, only one very important contribution it is observed for the hydrochloride species from an antibonding to antibonding orbital, $\pi^*C9\text{-}C15 \rightarrow \pi^*C5\text{-}C11$. On the other hand, the cationic species present other different transitions not observed in the other two species, as can be seen in Table 6. The calculated total energy favors clearly to the hydrochloride species with a highest energy value than the other ones. Besides, the total energy for the free base is practically similar to that observed for the cationic species, suggesting thus, that both forms have basically the same stabilities.

In this study, for the three species were calculated the topological properties by using the Bader's theory and the AIM2000 program [28,42] in the gas phase and with the B3LYP/6-311++G** level of theory. This way, for those three species of DPH were computed the electron density, $\rho(r)$, the Laplacian values, $\nabla^2\rho(r)$ and, the eigenvalues $(\lambda1, \lambda2, \lambda3)$ of the Hessian matrix and the $\lambda1/\lambda3$ ratio in the Bond Critical Points (BCPs) and Ring Critical Points (RCPs). Thus, these results for the free base, cationic and hydrochloride species are presented in **Tables 6, 7** and **8**, respectively. Here, it is necessary to clarify that when in an interaction there are high values of $\rho(r)$ and $\nabla^2\rho(r)$, the ratio $\lambda1/\lambda3 > 1$ and $\nabla^2\rho(r) < 0$, this interaction is covalent (named shared interaction) and, the interaction is named ionic or highly polar covalent if $\lambda1/\lambda3 < 1$ and $\nabla^2\rho(r) > 0$ (closed-shell interaction). The results for the free base and cationic show that there is a new RCP, named RCPN1 as a consequence of the H bonds formed in both species. Note that the nature or characteristic of those bonds are very different between them, thus, in the free base the H bond is formed between two H atoms (H22---H29) while in the cationic species the H bond is formed between the O and H atoms (O1---H41). Then, their properties are also very different, having higher values the O1---H41 bond, as expected because this bond is formed by atoms of different electronegativities and, besides, the distance is short between both atoms.

Table 6. Analysis of the Bond Critical Points (BCPs) and Ring Critical Points (RCPs) for the free base of diphenhydramine in gas phase by using B3LYP/6-311++G** level of theory.

B3LYP/6-311++G** method				
Parameter[#]	RCP1	RCP2	RCPN1	H22---H29
$\rho(r)$	0.0218	0.0219	0.009	0.0099
$\nabla^2\rho(r)$	0.1598	0.1599	0.042	0.0364
$\lambda1$	-0.0857	-0.0864	-0.003	-0.0029
$\lambda2$	-0.0911	-0.0904	-0.047	-0.0492
$\lambda3$	0.1855	0.1880	0.1827	0.1910
$\lvert\lambda1\rvert/\lambda3$				
Distance				2.165

[#]The quantities are in atomics units and distances in Å

Table 7. Analysis of the Bond Critical Points (BCPs) and Ring Critical Points (RCPs) for the cationic species of diphenhydramine in gas phase by using B3LYP/6-311++G** level of theory.

B3LYP/6-311++G** method				
Paramet[#]	RCP1	RCP2	RCPN1	O1---
$\rho(r)$	0.0218	0.0218	0.0232	0.0274
$\nabla^2\rho(r)$	0.1596	0.1596	0.1412	0.1090
$\lambda1$	-	-0.0170	-0.0232	-0.0345
$\lambda2$	0.0860	0.0863	0.0393	-0.0293
$\lambda3$	0.0906	0.0905	0.1250	0.1729
$\|\lambda1\|/\lambda3$	0.1865	0.1878	0.1856	0.1995
Distanes				1.971

[#]The quantities are in atomics units and distances in Å

Table 8. Analysis of the Bond Critical Points (BCPs) and Ring Critical Points (RCPs) for the hydrochloride species of diphenhydramine in gas phase by using B3LYP/6-311++G** level of theory.

B3LYP/6-311++G** method				
RCPs				
Paramet er[#]	RCP1	RCP2	RCPN3	RCPN4
$\rho(r)$	0.0218	0.0219	0.0103	0.0039
$\nabla^2\rho(r)$	0.1598	0.0159	0.0474	0.0137
$\lambda1$	-0.0169	-0.0170	-0.0044	-0.0021
$\lambda2$	0.0861	0.0865	0.0050	0.0033
$\lambda3$	0.0906	0.0902	0.0468	0.0125
$\|\lambda1\|/\lambda3$	0.1630	0.1885	0.0940	0.1680
BCPs				
Paramet er[#]	O1--- H29	Cl42--- H28	Cl42--- H41	
$\rho(r)$	0.0108	0.0083	0.0770	
$\nabla^2\rho(r)$	0.0397	0.0239	0.0321	
$\lambda1$	-0.0089	-0.0065	-0.1276	
$\lambda2$	-0.0059	-0.0063	-0.1274	
$\lambda3$	0.0546	0.0368	0.2873	
$\|\lambda1\|/\lambda3$	0.1630	0.1766	0.4441	
Distance	2.472	2.769	1.754	

[#]The quantities are in atomics units and distances in Å

Analyzing the hydrochloride species, we observed different H and halogen bonds due to the presence of the Cl atom in this species. Thus, Table 9 shows clearly three new interactions, one the O1---H29 bond and the other two halogen Cl42---H28 and Cl42---H41ones. Notice that the topological properties are higher in the halogen Cl42---H41 bonds due to the short distance between both atoms. **Figure 5** show clearly those BCPs and RCPs for the hydrochloride species.

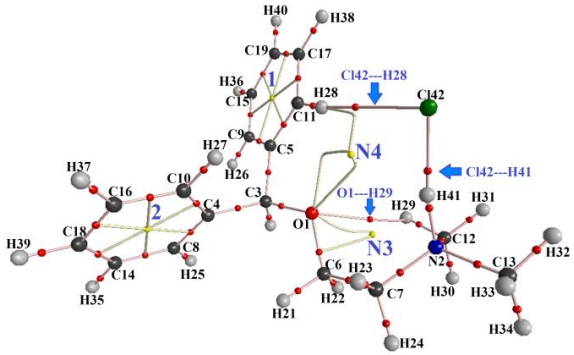

Figure 5. Details of the molecular model for the hydrochloride species of DPH in gas phase showing the geometry of all their bond critical points (BCPs) and ring critical points (RCPs) at the B3LYP/6-311++G** level of theory.

Frontier orbitals and global descriptors

The gap values, defined as the difference between the HOMO and LUMO orbitals, and some quantum chemical descriptors are very interesting parameters to predict the reactivities and behaviours of many species, as suggested by Parr and Pearson [29]. In this work, we have calculated these parameters for the free base, cationic and hydrochloride species of DPH in the gas phase by using the B3LYP/6-311++G** level of theory. Hence, the species is reactive when the gap values between both frontier orbitals are very closer and, on the contrary, when the distances between the two orbitals are longer the molecule is less reactive. On the other hand, the chemical potential (μ), electronegativity (χ), global hardness (η), global softness (S), global electrophilicity index (ω) and global nucleophilicity index (E) descriptors are calculated from the corresponding gap values by using known equations [30-36]. Here, the frontier orbitals and gap values for those three species of DPH can be seen in **Table 9** together with the descriptors and their equations.

Table 9. The frontier molecular HOMO and LUMO orbitals and some descriptors for the free Base, cationic and diphenhydramine in gas phase by using B3LYP/6-311++G** level of theory.

B3LYP/6-311++G**			
Orbital	Gas phase		
(eV)	Free base	Cationic	HCl
HOMO	-5.9497	-9.2872	-6.0830
LUM	-0.6383	-3.9114	-0.8277
GAP	5.3114	5.3758	5.2554
Descriptors			
(eV)	Free base	Cationic	HCl
χ	-2.6557	-2.6879	-2.6277
μ	-3.2940	-6.5993	-3.4554
η	2.6557	2.6879	2.6277
S	0.1883	0.1860	0.1903
ω	2.0429	8.1014	2.2719
E	-8.748	-17.738	-9.080

$\chi = -[E(LUMO) - E(HOMO)]/2$; $\mu = [E(LUMO) + E(HOMO)]/2$; $\eta = [E(LUMO) - E(HOMO)]/2$; $S = \frac{1}{2}\eta$; $\omega = \mu^2/2\eta$

• • • • •

The gap values clearly show that the hydrochloride form is the most reactive because it species present lower gap value while, contrarily to the expected, the cationic form is the less reactive. Here, the comparisons among these three-species containing two N-CH_3 groups with the tropane alkaloids which present only a group are very interesting to know how affect these two groups to the reactivity values. This way, in **Table 10** are compared these values for three different alkaloids [37-39]. The analysis exhaustive of the gap values for all free bases of these alkaloids, including the DPH species, show that the higher value is observed for tropane alkaloid while the lower value for cocaine, therefore, this latter species is the most reactive. For the cationic species, tropane alkaloid is the less reactive while morphine is the most reactive. Note that the three curves present similar behaviors for the three forms of the four species, as can be seen in **Figure 6**. Evaluating the hydrochloride species, tropane is the less reactive while cocaine is the most reactive.

On the other hand, the chemical potential (μ), electronegativity (χ), global hardness (η), global softness (S), global electrophilicity index (ω) and global nucleophilicity index (E) descriptors values for all free base, cationic and hydrochloride forms of the three tropane alkaloids are presented in Table 11 and their behaviors, together with those observed for DPH, are analyzed graphically in **Figure 7**.

Table 10. Gap values and some descriptors for the free Base. cationic and hydrochloride species of DPH in gas phase compared with the corresponding to tropane, cocaine and morphine species.

Tropane alkaloids			
Orbital	B3LYP/6-31G*		
|GAP|	Gas phase		
(eV)	Free base	Cationic	HCl
Tropane	7.5506	9.5595	6.8246
Cocaine	4.8580	5.4468	4.5082
Morphine[c]	5.6044	5.1889	5.4417
Descriptors			
Tropane[a]			
(eV)	Free	Cationic	HCl
χ	-3.7753	-4.7798	-3.4123
μ	-1.7192	-8.1567	-2.1787
η	3.7753	4.7798	3.4123
S	0.1324	0.1046	0.1465
ω	0.3914	6.9598	0.6955
E	-6.4905	-38.9872	-7.4343
Cocaine[b]			
(eV)	Free base	Cationic	HCl
χ	-2.4290	-2.7234	0.5647
μ	-3.4977	-6.5928	-0.6209
η	2.4290	2.7234	0.5647
S	0.2058	0.1836	0.8854
ω	2.5183	7.9799	0.3413
E	-8.4959	-17.9548	-0.3506

Morphine[c]			
(eV)	Free	Cationic	HCl
χ	-2.8022	-2.5945	-2.7209
μ	-2.7648	-5.9469	-3.1709
η	2.8022	2.5945	2.7209
S	0.1784	0.1927	0.1838
ω	1.3639	6.8155	1.8476
F	-7.7475	-15.4288	-8.6274

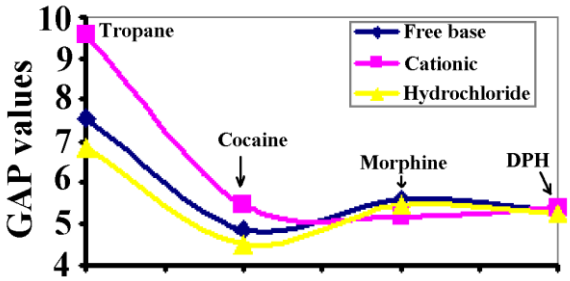

Figure 6. Comparisons of descriptors for the three species of DPH in gas phase at the B3LYP/6-311++G** level of theory with those reported for the free base, cationic and hydrochloride forms of tropane, cocaine and morphine at B3LYP/6-31G* level of theory [37-39].

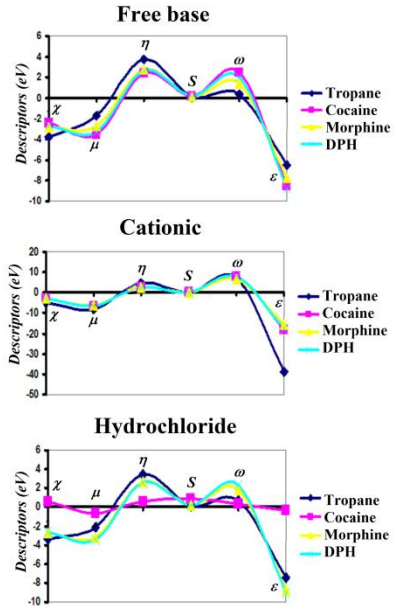

Figure 7. Comparisons of descriptors for the three species of DPH in gas phase at the B3LYP/6-311++G** level of theory with those reported for the free base, cationic and hydrochloride forms of tropane, cocaine and morphine at B3LYP/6-31G* level of theory [37-39].

Firstly, the analysis of the graphic for all free bases show that practically the same behaviors for all free bases, but χ is higher in cocaine than the other ones probably due to their higher electrophilicity index (ω) and low

nucleophilicity index. Later, it is observed for the four species practically the same *S* values while the higher η is observed for tropane, as expected because it has low reactivity. If now the cationic species of those four samples are evaluated, we observed a similar behavior for all species and, only for tropane it is observed the lowest nucleophilicity value. In relation to all hydrochloride species, it is observed that cocaine; morphine and DPH present nearly the same behaviors with exception of cocaine that shows approximately the same low descriptors values. These studies do not show significant differences among the three DPH species and those corresponding to tropane alkaloids and, as a consequence the two N-CH_3 groups basically don't have influence on the descriptors but if on the reactivities of their three species.

Vibrational analysis

The free base, cationic and hydrochloride species of DPH in the gas phase were optimized with C_1 symmetries by using the B3LYP/6-311++G** level of theory. For the free base are expected 114 normal vibration modes while for the cationic and hydrochloride species 117 and 120 modes, respectively. All these modes have activities in both IR and Raman spectra. The predicted infrared spectra for those three species in gas phase can be observed in **Figure 8** compared with the corresponding experimental available for the hydrochloride species de DPH from Ref [46] while the predicted Raman spectra for those three species of DPH are presented in **Figure 9**. Here, some experimental IR bands were also taken of other IR spectrum reported for that DPH species from Ref [47]. Some bands observed in the experimental available Raman spectrum for the hydrochloride DPH in the region 2000-400 cm^{-1} were taken from Ref [48] and due to the low quality of that spectrum it cannot be presented in figure 9.

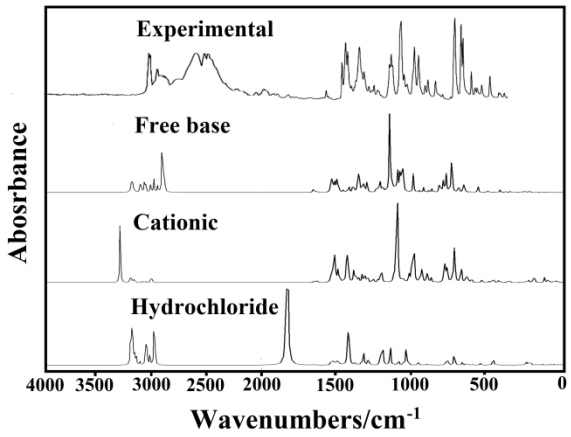

Figure 8. Predicted infrared spectra for free base, cationic and hydrochloride forms of DPH compared with the corresponding experimental for the hydrochloride species from Ref. [46].

Figure 8 shows that: (i) the better correlations can be observed for the free base and the cationic forms of DPH and, (ii) the hydrochloride form is not present in the solid phase or probably is in a low proportion because the strong IR band predicted at 1818 cm^{-1} is not observed in the experimental IR spectrum. This strong band is associated to the N-H stretching linked to Cl atom (N-H---Cl). In this work, the predicted Raman spectra for the three species of DPH in activities were converted to intensities by using recommended equations [43,44]. The harmonic force fields for those three species of DPH were computed with the SQMFF approach [25], the corresponding normal internal coordinates and the Molvib program [26]. Despite the scale factors used here in the refinement process were reported for B3LYP/6-31G* calculations, in this work, we also have employed these values [25] for our B3LYP/6-311++G** calculations. Potential energy distribution (PED) contributions $\geq$ 10% were used to perform the vibrational assignments for all species. Afterwards, in **Table 11** are given the observed and calculated wavenumbers together with their corresponding assignments in the gas phase at the B3LYP/6-311++G** level of theory.

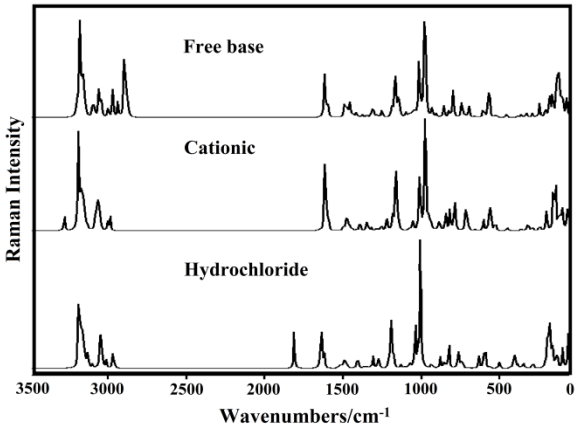

Figure 9. Predicted Raman spectrum for free base, cationic and hydrochloride forms of DPH in gas phase by using the B3LYP/6-311++G** level of theory.

Table 11. Observed and calculated wavenumbers (cm^{-1}) and assignments for the Free Base, Cationic and Hydrochloride forms of Diphenhydramine in gas phase.

Experimental		B3LYP 6-311++G**[a]					
		Free base		Cationic		Hydrochloride	
IR[c,d]	Rama	SQM[b]	Assignment[a]	SQ	Assignment[a]	SQM	Assignment[a]
				315	νN2-H41		
3062		3067	νC11-H28	306	νC18-H39		
		3060	νC18-H39	306	νC19-H40		
		3058	νC19-H40	305	νC10-H27	3058	νC16-H37
				305	νC15-H36	3056	νC17-H38
		3052	νC14-H35	305	νC14-H35	3051	νC10-H27
		3048	νC15-H36	304	νC11-H28	3047	νC15-H36
		3045	νC10-H27	304	νC16-H37	3042	νC14-H35
3040s		3040	νC17-H38	304	ν_aCH_3(C12)	3041	νC11-H28
		3038	νC16-H37	303	νC17-H38	3035	ν_aCH_3(C12)
		3034	νC9-H26	303	ν_aCH_3(C13)	3033	νC18-H39
		3033	νC8-H25	303	ν_aCH_3(C12)	3032	νC19-H40
				303	νC9-H26		
				302	ν_aCH_3(C13)	3025	ν_aCH_3(C13)
3026				302	νC8-H25	3020	νC8-H25
				301	ν_aCH_2(C7)	3019	νC9-H26
3000s		2991	ν_aCH_3(C12)			3007	ν_aCH_3(C13)
2991s		2981	ν_aCH_3(C13)			3002	ν_aCH_3(C12)
2960s		2952	ν_aCH_3(C12)	296	ν_sCH_2(C7)	2976	ν_aCH_2(C7)
		2945	ν_aCH_2(C7)	294	ν_sCH_3(C12)		
2931s		2941	ν_aCH_3(C13)	294	ν_sCH_3(C13)	2926	ν_sCH_3(C13)
2902		2919	ν_aCH_2(C6)	293	ν_aCH_2(C6)	2920	ν_sCH_3(C12)
		2897	νC3-H20	288	νC3-H20	2914	ν_sCH_2(C7)
2879s		2889	ν_sCH_2(C6)			2889	ν_aCH_2(C6)
2875s				287	ν_sCH_2(C6)		
						2851	νC3-H20

2850s						2842	$\nu_s CH_2$(C6)
		2823	$\nu_s CH_3$(C13)				
		2818	$\nu_s CH_3$(C12)				
		2806	$\nu_s CH_2$(C7)				
1696						1748	νN2-H41
				159	νC9-C15,νC11-	1590	νC9-C15
		1584	νC9-C15	158	νC10-C16	1585	νC10-C16
1600 w		1580	νC10-C16	157 3	νC14-C18, νC16-C18,νC4-C8	1572	νC14-C18,νC16-C18,νC4-C8
1581v w		1568	νC14-C18,νC16-C18	157 1	νC15-C19, νC17-C19	1569	νC15-C19,νC17-C19
		1566	νC15-				
1492s		1474	βC15-H36	148	βC15-H36	1481	βC15-H36
		1473	βC16-H37	147	βC14-H35	1477	βC14-H35
1468v	1468w			146	βC12-H31	1465	βC12-H31
1463s				146	δCH_2(C6)		
1454v	1456w			145	$\delta_a CH_3$(C13)	1453	δCH_2(C6)
1443s	1446w	1449	δCH_2(C6)	144	$\delta_a CH_3$(C13)	1452	ρ'N2-H41, $\delta_a CH_3$(C13)
		1440	$\delta_a CH_3$(C13)	144	βC18-H39	1441	$\delta_a CH_3$(C12), βC18-H39
1430	1436w	1437	βC14-H35	144	βC19-H40	1440	$\delta_a CH_3$(C12) ,βC18-H39
		1432	βC19-	143	δCH_2(C7)	1436	βC19-H40
		1431	$\delta_a CH_3$(C12)			1428	$\delta_a CH_3$(C12)
1424s		1424	$\delta_a CH_3$(C13)	142	βC12-	1421	$\delta_a CH_3$(C13)
		1418	βC12-H31	141 5	βC12-H31,$\delta_s CH_3$(C12)	1417	ρN2-H41
1412s		1411	$\delta_a CH_3$(C13)	141	δCH_2(C7)	1413	$wagCH_2$(C6)
1402		1406	$wagCH_2$(C6)	139	$wagCH_2$(C6)	1409	δCH_2(C7)
1399s		1396	δCH_2(C7)	138	$\delta_s CH_3$(C13)	1385	$wagCH_2$(C7)
		1380	$wagCH_2$(C7)	138	$\delta_a CH_3$(C12),$\delta_s CH_3$(		
1376v s		1377	$\delta_a CH_3$(C12) $\delta_s CH_3$(C13)			1375	$\delta_s CH_3$(C13)
1364	1361w					1366	$\delta_a CH_3$(C12),νN2-H41
1345v		1347	ρ'C3-H20	134	$wagCH_2$(C7),ρN2-		
		1342	ρC3-H20	134	ρC3-H20	1340	ρC3-H20
1327				133	ρ'C3-H20,βC9-H26	1333	βC9-H26
1319s		1311	βC9-H26	131	ρ'C3-H20	1315	ρ'C3-H20
1303		1302	βC8-H25	130	C10-C16	1302	C10-C16
1293		1295	ρCH_2(C7)	128	νC5-C11	1287	ρCH_2(C7)
1279		1275	C5-C11	127	ρCH_2(C7)	1274	νC5-C11
1260	1297w	1261	ρCH_2(C6)				
1246	1255w	1245	νC4-C10	124	νC4-C10	1246	ρC3-H20, ρCH_2(C6)
1230		1241	βC12-H29	122	ρCH_2(C6),ρCH_3(C1	1241	ρCH_2(C6)
	1218			121	ρCH_3(C12)	1229	ρCH_3(C12) ,ρCH_3(C13)
1180s	1181w	1180	νC3-C5, νC5-C9	118	νC3-C5,νC5-C9	1176	νC3-C5,νC5-C9
1168s				117 2	βC16-H37, βC10-H27,βC8-H25	1173	βC17-H38, βC11-H28,νC11-C17
1168s		1165	βC13-H32,	116	βC13-H32	1168	βC16-H37, βC10-
1164s		1161	νC3-C4	116	βC13-H32	1164	νC3-C4
		1158	βC10-H27	116	νC3-C4	1164	βC13-H32 ,βC12-H29
		1157	ρ'C12-H30	115	βC18-H39	1149	βC18-H39
1153		1156	βC11-	115	βC19-H40,βC17-	1148	βC19-H40

		1138	βC18-H39			1140	ρ'C12-H30
		1136	βC19-H40	113	ρ'C12-H30		
1114v		1096	ρ'CH_3(C13)			1094	νC6-O1, νC6-C7
1110v	1100w	1074	νC3-O1	107	νC8-C14, νC9-C15	1079	νC9-C15, νC11-C17
1088s	1085w	1062	νC6-C7	106	νC8-C14	1065	νC8-C14
1069		1059	νC8-C14				
1055s				105	νC6-O1,νC6-C7	1053	ρ'CH_3(C13)
	1035	1026	ρCH_3(C13)	103	ρ'CH_3(C13)	1020	βR_1(A1)
1022v		1019	νC6-O1	101	βR_1(A2)	1019	γC11-H28, νC6-C7
		1015	βR_1(A1)	101	βR_1(A1)	1018	γC11-H28, γC17-H38
		1013	βR_1(A2)	101	τ$_w$$CH_2$(C6)	1016	γC11-H28, γC17-H38
		1005	γC17-H38	100	γC18-H39,γC16-	1016	ρCH_3(C13)
		1003	γC18-H39	1005	γC19-H40,γC15-H36	1000	γC16-H37,γC18-H39
1001	1008v	1001	νC3-O1,νC13-	997	βR_1(A2), βR_1(A1)	997	νC3-O1
991m		994	νC13-N2	995	βR_1(A2), βR_1(A1)	995	βR_1(A2)
		993	βR_1(A1), βR_1(A2)			991	νC3-O1
		988	γC15-H36	982	γC14-H35	982	γC15-H36
		987	νC3-O1	980	γC11-H28	979	γC14-H35
	970w	986	γC14-H35	973	δC7C6O1	971	νC13-N2, τ$_w$$CH_2$(C6)
958m				951	νC3-O1		
949m	945w	936	γC8-	947	νC13-N2,	938	γC19-H40
928m		927	γC11-H28	929	γC8-H25	925	γC10-H27
		920	νC12-N2	924	γC9-H26		
	892m			892	νC12-N2	904	νC12-N2
880m		861	δO1C3C5	863	νC5-C11		
852w	855m	852	γC9-H26			855	δO1C3C5
		850	γC10-H27,γC16-	850	γC9-H26	854	γC9-H26
				845	γC10-H27	849	γC8-H25
831w		830	τ$_w$$CH_2$(C7)	833	τ$_w$$CH_2$(C7)	839	τ$_w$$CH_2$(C7)
	820m	825	δC4C3C5	822	δC4C3C5	825	νC4-C10
786w	765w	761	νC7-N2	763	τR_1(A1)	756	τR_1(A1)
758vs		756	τR_1(A1)	748	τR_1(A2)	746	νC7-N2
		746	τR_1(A2),γC19-			743	τR_1(A2), γC19-H40
715vs				726	νC7-N2		
699vs		698	τR_1(A2)	700	τR_1(A2) ,τR_1(A1)	701	τR_1(A2)
		692	τR_1(A1),τR_1(A2)	692	τR_1(A2), τR_1(A1)	692	τR_1(A1), τR_1(A2)
644m	650m	655	βR_3(A1)	657	βR_3(A1)	654	βR_3(A1)
	630m	632	βR_2(A2)	633	βR_2(A2)	632	βR_2(A2)
621w		627	βR_2(A1)	629	βR_2(A1)	629	βR_2(A1)
609w		619	βR_3(A2)	620	βR_3(A2)	618	βR_3(A2)
577m		586	δC7C6O1	589	δC7C6O1	586	δC7C6O1
	515m	538	τR_2(A1)	518	τR_2(A1)	532	τR_2(A1)
470w	473w	471	τR_2(A2)	472	τR_2(A2)	469	τR_2(A2)
459w		458	δC12N2C13	449	δC12N2C13	449	δC7N2C12
434w	430w	427	δC7N2C12			431	δC12N2C13
411w		413	δC7N2C13	411	δC7N2C12		
		401	τR_3(A2)	400	τR_3(A2)	401	τR_3(A2) ,τR_2(A1)

398	τR_3(A2), τR_3(A1)	398	τR_3(A1)	400	τR_3(A1)
348	δC7N2C13	385	δC7N2C13	397	τR_3(A2)
		347	δC7N2C12	350	δC7C6O1
315	δC6C7N2	307	δC7N2C13,βC3-C5		
286	$\tau_w CH_3$(C12)			290	δC7N2C13, βC3-C5,
265	βC3-	269	βC3-C4	267	τC6-C7,βC3-C5
259	τR_3(A1)	256	τR_3(A1), δC6C7N2	256	τC6-C7
240	τwCH_3(C13)			252	τR_3(A1), τR_2(A1)
228	βC3-C4	231	τC6-C7	228	νH41-Cl42
213	$\tau_w CH_3$(C12)	216	βC3-C4	219	βC3-C4, δO1C3C4
		209	$\tau_w CH_3$(C13)	205	$\tau_w CH_3$(C13),νH41-Cl42
180	τ_wC3-O1	177	τR_3(A1)	192	$\tau_w CH_3$(C13),τ_wCH3(C12)
		175	$\tau_w CH_3$(C12)	170	τR_3(A1), τ_wC3-O1
135	τ_wC7-N2, τC6-			135	τ_wC7-N2, δN2H41Cl42
98	τ_wC7-N2, τC6-	109	τ_wC7-N2δ	114	δN2H41Cl42
88	τ_wC3-O1	86	δC3O1C6,δO1C3C	82	δC3O1C6
				65	τN2-H41,τ_wC3-O1
58	δC4C3C5 γC3-	57	γC3-C4,γC3-C5	56	δC4C3C5,γC3-C4,γC3-
49	τC6-O1	46	τ_wC7-N2δ	50	τ_wC7-N2
39	τC6-O1	41	τ_wC3-C5	42	τ_wC3-C5
33	τ_wC3-C5	31	τ_wC3-O1	36	τ_wC3-C4
19	τ_wC3-C4	23	τ_wC3-C4	27	τC6-O1
		16	τC6-O1		
				9	τ_wC3-C5 ,τ_wC7-N2

Abbreviations: ⋅, stretching; ⋅ ⋅ ⋅ deformation in the plane; ⋅ ⋅ ⋅ deformation out of plane; wag, wagging; ⋅ ⋅ ⋅ ⋅ torsion; β_R, deformation ring τ_R, torsion ring; ρ, rocking; τw, twisting; δ, deformation; a, antisymmetric; s, symmetric, [a]This work, [b]From scaled quantum mechanics force field; [c]From Ref [46]; [d]From Ref [47]; [e]From Ref [48].

Analyzing the experimental available Raman spectrum for the hydrochloride form of DPH in the 2000-400 cm^{-1} region, in accordance to Ref [48], it is observed two bands with different intensities, one of them, of low intensity at 1035 cm^{-1} and the other one very strong at 1008 cm^{-1} while in the IR predicted spectrum the band of low intensity is located at 1052 cm^{-1} while the other one at 1020 cm^{-1}. These two bands are clearly attributed to one of the deformation ring modes of both phenyl rings R1 and R2. Thus, the first deformation ring modes is associated to R1 (βR_1(A1)) while the other deformation mode is attributed to ring R2, which is clearly predicted at 995 cm^{-1} ((βR_1(A2)). This greater separation between both deformation ring modes, R1 and R2, obviously, is attributed to the proximity of Cl atom to R2 and, as a consequence of the formation of bond Cl42---H28 halogen predicted by the AIM study. Evidently, the Cl atom generate the increases in the intensity of that band attributed to βR_1(A2).

Analyzing carefully the predicted IR spectrum of hydrochloride form in the 2000-400 cm^{-1} region we can see a very intense band at 1033 cm^{-1} which is attributed to one of the two C3-O1 stretching modes while the e two deformation rings βR_1(Aq2) and βR_1(A2) modes are predicted practically in the same positions (1016 and 1014 cm^{-1}, respectively), different from those positions observed in the Raman spectra. When the SQM methodology was employed the two C3-O1 stretching modes are predicted at 997/991 cm^{-1}. Subsequently, the assignments for some groups are presented at continuation.

Band Assignments

N-H modes. Obviously, only the NH stretching modes for the cationic and hydrochloride forms are expected in DMH. In some compounds, such as in the monomeric species of clonidine hydrochloride [49] the NH stretching modes were assigned at 3427/3341 cm^{-1} while in its dimer due to H bonds formation these stretching modes are shifted toward lower wavenumbers and, for this reason, the broad band observed at 2584 cm^{-1} it is assigned to those modes. In the cationic form of DPH, the N-H stretching mode is predicted by SQM calculations at 3150 cm^{-1} while in the hydrochloride form at 1748 cm^{-1}. On the other hand, in the experimental available IR spectra of the hydrochloride form [46,47] the set of broad bands in the 2756-2178 cm^{-1} region, with strong bands located at 2587, 2513 and 2482 cm^{-1}, can be easily assigned to the N-H stretching modes due to H bonds, as observed in the dimeric form of clonidine hydrochloride [49]. The two expected N-H rocking modes for the cationic and hydrochloride forms are predicted in different regions by SQM calculations. Accordingly, in the cationic species those modes are predicted at 1415 and 1348 cm^{-1} while in the hydrochloride form at 1452 and 1417 cm^{-1}. Subsequently, these modes were assigned in the 1452-1348 cm^{-1} region.

C-H modes. For the three species of DPH are expected ten aromatic C-H stretching modes where the C atoms have sp^2 hybridizations while only for the C3-H20 stretching mode the C atom presents sp^3 hybridization. Therefore, the aromatic C-H stretching modes are assigned to higher wavenumbers than the other aliphatic one, as can be observed in Table 11. Then, the in-plane and out-of-plane deformation modes only can be expected for the CH groups with sp^2 hybridizations of the three species in the 1481/1148 and 1019/746 cm^{-1} regions, respectively while for the C3-H20 groups of the three species are expected two rocking and three deformation modes, as shown in Table 11. Thus, all these vibration modes are assigned to the IR and Raman bands observed in the regions predicted by SQM calculations.

CH_3 modes. For the three species of DPH are expected a total of 18 vibration normal due to the two CH_3 groups present in the free base, cationic and hydrochloride forms. Generally, in species containing these groups, the antisymmetric and symmetric modes are assigned between 3000 and 2900 cm^{-1} [30-34,36-39] showing the symmetric modes very intense Raman bands. Here, these stretching modes in the free base, cationic and hydrochloride species are predicted in the 2991/2942, 3041/2942 and 3035/2920 cm^{-1}, respectively and, for these reasons, they are assigned in these regions. Note the shifting of bands assigned to these modes in the hydrochloride species toward lower wavenumbers due to the presence of Cl atom. In different species, the deformation CH_3 modes are predicted between 1485 and 1377 cm^{-1} while the rocking modes between 1049 and 1007 cm^{-1} and the twisting modes between 45 and 20 cm^{-1} [30-34,36-39]. In the three species of DPH these modes are predicted in approximately the same regions. Thus, the deformation modes in the free base, cationic and hydrochloride species are predicted by SQM calculations in the 1440/1377, 1450/1382 and 1452/1366 cm^{-1} regions, the rocking modes in the 1096/1026, 1220/1034 and 1229/1016 cm^{-1} regions, while the twisting modes in the 240/213, 209/175 and 205/195 cm^{-1} regions, respectively. Hence, these vibration modes are assigned in accordance to these predictions and, as indicated in Table 11.

CH_2 modes. The three species of DPH have two CH_2 groups and, for these reasons, twelve vibration modes are expected in each of those forms. This way, the antisymmetric and symmetric stretching modes are predicted by SQM calculations for the free base, cationic and hydrochloride species between 2945/2806, 3014/2872 and 2976/2842 cm^{-1}, respectively, therefore, the IR bands observed in those regions can be easily assigned to these vibration modes. The other modes related to these groups, such as the deformation, wagging, rocking and twisting modes were predicted for the free base, cationic and hydrochloride species in different regions, as observed in Table 12. Hence, the deformation modes are predicted in the free base, cationic and hydrochloride species at 1449/1396, 1460/1412, and 1453/1409 cm^{-1} regions, respectively while the corresponding wagging modes at 1406/1380, 1398/1348 and 1413/1385 cm^{-1} regions, respectively. The rocking and twisting modes expected for the three species of DPH were predicted for the free base at 1295/1261 and 936/839 cm^{-1}, for the cationic species at 1270/1220 and 947/833 cm^{-1}, and for the hydrochloride form at 1287/1241 and 971/839 cm^{-1}. Consequently, these vibration modes were clearly associated to the IR and Raman bands observed in those regions.

4.5.1. Skeletal modes. The C=C stretching modes corresponding to the two diphenyl rings in the three species of DPH were predicted between 1590 and 1566 cm^{-1}, hence, they were easily assigned to the weak IR bands at 1600 and 1581 cm^{-1} while the C-C stretching modes are predicted in different regions, thus, the C3-C5 and C5-C9 stretching modes are predicted at higher wavenumbers (1182-1176 cm^{-1}) than the C3-C4 stretching modes (1164-1161 cm^{-1}) and, as a consequence they were assigned in these regions. The C3-O1 stretching mode is predicted in the free base at higher wavenumbers than the other C6-O1 stretching mode, that is, 1074 and 1019 cm^{-1}, respectively but, in the cationic and hydrochloride species, the C6-O1 stretching modes are predicted at higher wavenumbers than the other C3-O1 stretching ones. Thus, the C6-O1 and C3-O1 stretching in the cationic form are predicted at 1051 and 951 cm^{-1}, respectively while in the hydrochloride form these modes are predicted at 1094 and 997/991 cm^{-1}. Here, the presence of H atom in the cationic form and the H and Cl atoms in the hydrochloride forms justify clearly those differences observed in the positions of both stretching modes. Analyzing the positions of the two N2-CH_3 stretching modes, we observed that in the three species the N2-C13 stretching modes are predicted at higher wavenumbers than the other N2-C12 ones, as observed in similar species [37-39]. This way, the separations between the wavenumbers observed for those two stretching modes in the free base, cationic and hydrochloride species are 81, 55 and 67 cm^{-1}, respectively. Evidently, the presence of H atom in the cationic form and, of H and Cl atoms in the hydrochloride species reduce the separations between those vibration modes. The other N2-C7 stretching modes are predicted in the free base, cationic and hydrochloride species at lower wavenumbers than the other two N-CH_3 stretching modes, that is, at 761, 726 and 746 cm^{-1}, respectively. Obviously, these stretching modes are affected by the H and Cl atoms in the cationic and hydrochloride species, respectively. The other skeletal modes, such as the deformation and torsion of both diphenyl rings were assigned in accordance to compounds containing these rings [30-32,34], as can be seen in Table 11.

Force constants

The harmonic force constants for the free base, cationic and hydrochloride forms of DPH were computed from the corresponding harmonic force fields calculated by using the B3LYP/6-311++G** level of theory with the SQMFF approach [25] and the Molvib program [26]. **Table 12** shows the values obtained for those three species of DPH compared with the corresponding to the three species of tropane, cocaine and morphine alkaloids by using the B3LYP/6-31G* method [37-39]. Analyzing first the *f(νN-H)* force constants for the cationic and hydrochloride species of DPH we observed that the constant of the cationic species is higher than the corresponding to the hydrochloride ones, as also was observed in the three alkaloids [37-39].

Table 12, Comparison of main scaled internal force constants for the Free Base, Cationic and Hydrochloride forms of Diphenhydramine in gas phase.

Force constants	B3LYP/6-311++G**[a]		
	Gas phase		
	Free base	Cationic	HCl
f(ν N-H)		5.49	2.69
f(νCH)R	5.10	5.10	5.14
f(ν N-CH3)	4.52	4.03	4.28
f(νCH2)	4.61	4.78	4.66
f(νCH3)	4.70	4.97	4.92
f(νC-C)	4.06	4.13	4.04
f(νC-C)R	6.31	6.36	6.35
f(νC-N)	4.42	4.09	4.23
f(νC-O)	4.30	4.24	4.53
B3LYP/6-31G* Method			
tropane[b]			
f(ν N-H)		5.97	2.70

f(ν N-CH₃)	4.69	4.09	4.42
f(ν C-N)	4.16	3.11	3.73
f(ν CH₂)	4.78	4.88	4.85
f(ν CH₃)	4.72	5.10	5.03
f(ν C-H)	4.78	4.92	4.90
f(ν C-C)	4.05	4.17	4.16
Cocaine[c]			
f(ν N-H)		4.91	3.23
f(ν N-CH₃)	4.69	4.17	4.31
f(ν C-N)	4.20	3.41	3.71
f(ν CH₂)	4.85	4.91	4.88
f(ν CH₃)	4.86	5.07	5.04
f(ν C-H)	4.86	4.93	4.91
f(ν C-C)	3.94	4.06	4.08
Morphine[d]			
f(ν N-H)		5.93	2.73
f(ν N-CH₃)	4.83	4.05	4.37
f(ν C-N)	4.74	3.67	4.20
f(ν CH₂)	4.69	4.85	4.82
f(ν CH₃)	4.70	5.08	5.01
f(ν C-H)	4.65	4.62	4.72
f(ν C-C)	5.74	6.04	5.79

Units are mdyn Å^{-1} for stretching and mdyn Å rad^{-2} for angle deformations, [a]This work, [b]From Ref [37]; [c]From Ref [39]; [c]From Ref [38].

The graphic of these constants from **Figure 10** shows clearly that the force constants for all hydrochlorides species are higher than the cationic ones, as expected, because the Cl atoms most electronegative produce an enlargement of the N-H bonds due to the new H---Cl bonds and, as a consequence generate reductions in the *f(νN-H)* force constants values. Note that the hydrochloride form of cocaine presents the higher *f(νN-H)* force constant while the cationic form of tropane present the higher value.

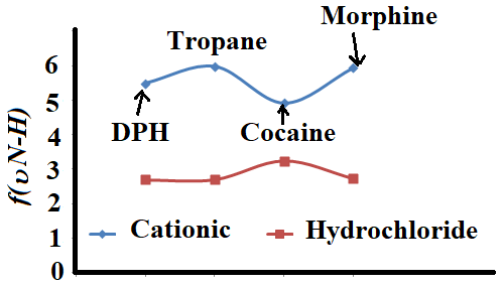

Figure 10. Comparisons among the f(νN-H) force constants for free base, cationic and hydrochloride forms of DPH in gas phase by using the B3LYP/6-311++G** level of theory with those calculated for the three forms of tropane, cocaine and morphine alkaloids by using the 6-31G* basis set.

If now, we analyze the *f(ν N-CH₃)* force constants for DPH and the alkaloids from **Figure 11**, we observed that the three species of DPH present the lower values despite their three forms have two N-CH₃ groups different from the alkaloids which have only one group. Here, morphine presents the higher value of all free base species, cocaine the higher value of all cationic forms while that the hydrochloride form of tropane presents the higher values than the other ones. Other very important constant to analyze is the *f(νC-C)$_R$* force constants related to the diphenyl rings that presents slightly the higher value in the cationic form of DPH than the other two ones. Probably, this fact is due to that in the hydrochloride form the Cl atom generates the formation of a Halogen bond with an H atom of one of the rings producing a decreasing in its value. The slight differences in the *f(νCH₂)*

and *f(νCH3)* force constants are related with the number of these groups and its positions, thus, in the alkaloids species the CH_2 groups are included in the rings.

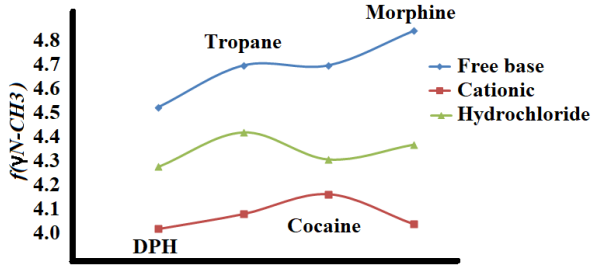

Figure 11. Comparisons among the f(νN-CH_3) force constants for free base, cationic and hydrochloride forms of DPH in gas phase by using the B3LYP/6-311++G** level of theory with those calculated for the three forms of tropane, cocaine and morphine alkaloids by using the 6-31G* basis set.

Conclusions

In this work, the structural and vibrational properties of the free base, cationic and hydrochloride forms of diphenhydramine (DPH) were theoretically studied in the gas phase by using the B3LYP/6-311++G** level of theory. The complete vibrational assignments for those three species were performed by using the experimental available IR and Raman spectra for the hydrochloride form in the solid phase with the SQMFF approach and the Molvib program. Hence, the 114, 117 and 120 vibration normal modes expected for the free base, cationic and hydrochloride species of DPH, respectively were reported together with their corresponding force fields at the B3LYP/6-311++G** level of theory. The atomic NPA and Mulliken charges, molecular electrostatic potentials, bond orders, main delocalization energies and topological properties were studied for those three species of DPH. The results show that the higher dipole moment value is observed for the cationic species, as expected because this species is charged while the presence of Cl atom justifies the higher volume observed for the hydrochloride species. Very good correlations were found between the theoretical and experimental available geometrical parameters for the hydrochloride species of DPH. The studies of both charges show that the effect of to add an H atom to the free base is to modify the sign on the N2 atom and increase its charge and, also the negative charges on the O1, C12 and C13 atoms. On the contrary, the effect of to add a Cl atom to the cationic species is to increase the charges on the N2 and C13 atoms and, to decrease the negative charges on the O1 and C12 atoms. The NBO and AIM analyses show that the hydrochloride species is the most stable than the other ones due to the presence of one H bond and two halogen bonds different from only one H bond observed in other two species of DPH. The evaluations of the frontier orbitals show that the hydrochloride form is the most reactive due to its low gap value while the cationic form is the less reactive. The comparisons of the gap values for the three species of DPH with other similar species containing the N-CH_3 groups, such as the tropane, cocaine and morphine alkaloids, have showed that the three species of DPH have practically the same reactivities while in the three forms of alkaloids the values are very different among them, presenting the three forms of tropane the lowest reactivities. Hence, the three species of DPH, with two N-CH_3 groups, have apparently the same reactivities than the cationic form of cocaine. The descriptors in the three species of DPH have shown similar behaviors than those observed in the corresponding to the alkaloids ones. The three species of DPH present the lower *f(νN-CH3)* force constants values than the tropane, cocaine and morphine alkaloids ones despite the species of DPH have two N-CH_3 groups different from the alkaloids which have only one group. Finally, the vibrational analyses for the three species of DPH evidence that the presence of two halogen bonds and one H bond in the hydrochloride species of DPH, due to the Cl atom, produce a shifting of deformation βR_1(A1) ring mode of a ring with respect to the other βR_1(A2) while in the free base and cationic are predicted at the same wavenumbers.

Acknowledgements.

This work was supported with grants from CIUNT Project N° 26/D207 (Consejo de Investigaciones, Universidad Nacional de Tucumán). The authors would like to thank Prof. Tom Sundius for his permission to use MOLVIB.

References

1. Glaser R, Maartmann-Moe K, X-Ray Crystallography Studies and CP-MAS 13C NMR Spectroscopy on the Solid-state Stereochemistry of Diphenhydamine Hydrochloride, an Antihistaminic Drug, J. Chem. Soc. Perkin Trans. 1990; 2:1205-1210.

2. Abdel Bade M. Spectrophotimetric Determination of Diphenhydramine Hydrochloride Using Carmisne y Solvent Extraction. Jour.Chem.Soc.Pak. 1993; 15(1):39-43.

3. Saxena M, Gaur S, Prathipati P, Saxena AK, Synthesis of some substituted pyrazinopyridoindoles and 3D QSAR studies along with related compounds: Piperazines, piperidines, pyrazinoisoquinolines, and diphenhydramine, and its semi-rigid analogs as antihistamines (H1), Bioorganic & Medicinal Chemistry. 2006; 14:8249–8258.

4. Orkoula MG, Kontoyannis CG, Markopoulou CK, Koundourellis JE. Quantitative analysis of liquid formulations using FT-Raman spectroscopy and HPLC. The case of diphenhydramine hydrochloride in Benadryl®. J Pharmaceutical and Biomedical Analysis. 2006; 41:1406–1411

5. Riahi S, Edris-Tabrizi F, Javanbakht M, Ganjali MR, Norouzi P, A computational approach to studying monomer selectivity towards the template in an imprinted polymer, J Mol Model. 2009; 15:829–836.

6. Jo S-H, Hong H-K, Chong SH, Lee HS, Choe H, H1 antihistamine drug promethazine directly blocks hERG K+ channel, Pharmacological Research. 2009; 60: 429–437.

7. Chartrand É, Arnold AA, Gravel A, Jenna S, Marcotte I, Potential role of the membrane in hERG channel functioning and drug-induced long QT syndrome, Biochim. Biophys. Acta. 2010; 1798:1651–1662.

8. Mishra AK, Kumar A, Mishra A. Development and validation of UV spectrophotometric method for estimation of diphenhydramine hydrochloride in soft gelatin capsule. IJPSR. 2010; 1(8):144-148.

9. Zayed MA, El-Habeebb AA. Spectroscopic study of structure of diphenhydramine drug and its products obtained via reactions with tetracynoethylene and iodine reagents and applications Drug Test. Analysis (2010).

10. Ge ZK, Luo YH, Zhao XY, Zhang YJ, Zhang H, Tia CC. Simultaneous determination of ibuprofen and diphenhydramine HCl in orally disintegrating tablets and its dissolution by reversed-phase high performance liquid chromatography (RP-HPLC). African Journal of Pharmacy and Pharmacology. 2011; 5(18):2100-2105.

11. Edebi VN, Ebeshi BU, Anganabiri E. Simultaneous assay of codeine phosphate and diphenhydramine hydrochloride in cough mixtures by zero-order derivative UV spectrophotometry. African Journal of Pure and Applied Chemistry. 2011; 5(5):104-110.

12. F. Estelle R. Simons, Keith J. Simons, Histamine and H1-antihistamines: Celebrating a century of Progress, J Allergy Clin Immunol 128(6) (2011) 1139-1150.

13. Gravel AE, Arnold AA, Dufourc EJ, Marcotte I, An NMR investigation of the structure, function and role of the hERG channel selectivity filter in the long QT syndrome, Biochimica et Biophysica Acta. 2013; 1828:1494–1502

14. Shahi S, Sonwane U, Zadbuke N, Tadwee I, Design and development of diphenhydramine hydrochloride topical liposomal drug delivery system, International Journal of Pharmacy and Pharmaceutical Sciences. 2013; 5(3):534-542.

15. Patel DM, Patel RJ, Shah HR, Patel CN. World Formulation and evaluation of diphenhydramine hydrochloride lozenges for treatment of Cough, Journal of Pharmacy and Pharmaceutical Sciences. 2014; 3(5):822-834.

16. Darwish HW, Metwally FH, Bayoumi AEL, Simultaneous spectrophotometric determination of diphenhydramine, benzonatate, guaifenesin and phenylephrine in their quaternary mixture using partial least squares with and without genetic algorithm as a powerful variable selection procedure, Digest Journal of Nanomaterials and Biostructures. 2014; 9(4):1359-1372.

17. Hassan SAU, Method Development of Diphenhydramine HCl (C17H21NO.HCl) On Spectrophotometer. IOSR Journal of Applied Chemistry. 2015; 8(3):59-62.

18. Sanchez A, Valverde A, Sinclair M, Mosley C, Singh A, Mutsaers AJ, Hanna B, Gu Y, Johnson R, The pharmacokinetics of DPH after the administration of a single intravenous or intramuscular dose in healthy dogs, J. Vet. Pharmacol. Therap. 2016; 39:452-459.

19. Hazell L, Raschi E, De Ponti F, Thomas SHL, Salvo F, Helgee EA, Boyer S, Sturkenboom M, Shakir S, Evidence for the hERG Liability of Antihistamines, Antipsychotics, and Anti-Infective Agents:A Systematic Literature Review From the ARITMO Project, The Journal of Clinical Pharmacology 2016, 00(0) 1–15.

20. Sanchez A, Valverde A, Sinclair M, Mosley C, Singh A, Mutsaers AJ, Hanna B, Johnson R, Gu Y, Beaudoin-Kimble M, Antihistaminic and cardiorespiratory effects of diphenhydramine hydrochloride in anesthetized dogs undergoing excision of mast cell tumors, JAVMA. 2017; 251(7):804-813.

21. Sube R, Ertel EA, Cardiomyocytes Derived from Human Induced Pluripotent Stem Cells: An In-Vitro Model to Predict Cardiac Effects of Drugs, J. Biomedical Science and Engineering. 2017; 10(11):527-549.

22. Lazny R, Ratkiewicz A, Nodzewska A, Wynimko A, Siergiejczyk L. Determination of the N-methyl stereochemistry in tropane and granatane derivatives in solution: a computational and NMR spectroscopic study, Tetrahedron Letters. 2012; 68 (31):6158-6163.

23. Becke AD, Density functional thermochemistry. Ⅲ. The role of exact exchange J. Chem. Phys. 1993; 98:5648-5652.

24. Lee C, Yang W, Parr RG, Development of the Colle-Salvetti correlation-energy formula into a functional of the electron density, Phys. Rev. 1988; B37:785-789.

a) Rauhut G, Pulay P, J. Phys. Chem. 1995; 99:3093-3099. b) *Correction:* Rauhut G, Pulay P, J. Phys. Chem. 1995; 99:14572.

25. Sundius T, Scaling of ab initio force fields by MOLVIB, Vib. Spectrosc. 2002; 29:89-95.

26. Chain F, Iramain MA, Grau A, Catalán CAN, Brandán SA, Evaluation of the structural, electronic, topological and vibrational properties of *N*-(3,4-dimethoxybenzyl)-hexadecanamide isolated from Maca (*Lepidium meyenii*) using different spectroscopic techniques, J. Mol. Struct. 2016; 1119:25-38.

27. Chain FE, Ladetto MF, Grau A, Catalán CAN, Brandán SA, Structural, electronic, topological and vibrational properties of a series of N-benzylamides derived from Maca (Lepidium meyenii) combining spectroscopic studies with ONION calculations, J. Mol. Struct. 2016; 1105:403-414.

28. Romani D, Tsuchiya S, Yotsu-Yamashita M, Brandán SA, Spectroscopic and structural investigation on intermediates species structurally associated to the tricyclic bisguanidine compound and to the toxic agent, saxitoxin, J. Mol. Struct. 2016; 1119:25-38.

29. Gatfaoui S, Issaoui N, Brandán SA, Roisnel T, Marouani H, Synthesis and characterization of p-xylylenediaminiumbis(nitrate). Effects of the coordination modes of nitrate groups on their structural and vibrational properties, J. Mol. Struct. 2018; 1151:152-168.

30. Romani D, Brandán SA, Structural, electronic and vibrational studies of two 1,3-benzothiazole tautomers with potential antimicrobial activity in aqueous and organic solvents. Prediction of their reactivities, Computational and Theoretical Chem. 2015; 1061:89-99.

31. Márquez MB, Brandán SA, A Structural and Vibrational Investigation on the Antiviral Deoxyribonucleoside Thymidine Agent in Gas and Aqueous Solution Phases, Int. J. Quantum Chem. 2014; 114:209-221.

32. Rudyk RA, Brandán SA, Force field, internal coordinates and vibrational study of alkaloid tropane hydrochloride by using their infrared spectrum and DFT calculations, Paripex A Indian Journal of Research. 2017; 6(8):616-623.

33. Brandán SA, Why morphine is a molecule chemically powerful. Their comparison with cocaine, Indian Journal of Applied Research. 2017; 7(7):511-528.

34. Romani D, Brandán SA, Vibrational analyses of alkaloid cocaine as free base, cationic and hydrochloride species based on their internal coordinates and force fields, Paripex A Indian Journal of Research. 2017; 6(9):587-602.

35. A.B. Nielsen, A.J. Holder, Gauss View 3.0, User's Reference, GAUSSIAN Inc., Pittsburgh, PA, 2000–2003.

36. Frisch, M.J. et al., GAUSSIAN 09, Revision A.02, Gaussian, Inc., Wallingford, CT, 2009.

37. Bader RFW, Atoms in Molecules, A Quantum Theory, Oxford University Press, Oxford, 1990, ISBN: 0198558651.

38. Keresztury G, Holly S, Besenyei G, Varga J, Wang AY, Durig JR, Vibrational spectra of monothiocarbamates - II. IR and Raman spectra, vibrational assignment, conformational analysis and ab initio calculations of S-methyl-N,N-dimethylthiocarbamate Spectrochim. Acta. 1993; 49A:2007-2026.

39. Michalska D, Wysokinski R, The prediction of Raman spectra of platinum(II) anticancer drugs by density functional theory, Chemical Physics Letters. 2005; 403:211-217.

40. Besler BH, Merz Jr KM, Kollman PA, Atomic charges derived from demiempirical methods, J. Comp. Chem. 1990; 11:431-439.

41. Available from Infrared Reference Spectrum. https://www.ssi.shimadzu.com/products/literature/ftir/a323.pdf

42. Available from Infrared Reference Spectrum.

43. https://webbook.nist.gov/cgi/cbook.cgi?ID=C58731&Mask=80#IR-SpecBass VC, The identification of sympathomimetic amines by Raman spectroscopy, Forensic Science. 1978; 11:57 – 65.

44. Romano E, Davies L, Brandán SA, Structural properties and FTIR-Raman spectra of the anti-hypertensive clonidine hydrochloride agent and their dimeric species, J. Mol. Struct. 2017; 1133:226-235.